

1 **A novel interplay between GEFs orchestrates Cdc42**
2 **activation in cell polarity and cytokinesis**

3

4 Brian Hercyk, Julie Rich, and Maitreyi Das[§]

5

6 Department of Biochemistry & Cellular and Molecular Biology, University of Tennessee,
7 Knoxville, TN, USA.

8 § Corresponding Author: mdas@utk.edu

9

10 **ABSTRACT**

11 The small GTPase Cdc42, a conserved regulator of cell polarity in eukaryotes, is activated by
12 two GEFs, Gef1 and Scd1, in fission yeast. Gef1 and Scd1 localize sequentially to the division
13 site to activate Cdc42 for efficient cytokinesis. The significance of multiple Cdc42 GEFs is not
14 well understood. Here we report a novel interplay between Gef1 and Scd1 that fine-tunes Cdc42
15 activation during two cellular programs: cytokinesis and polarized growth. We find that Gef1
16 promotes Scd1 localization to the division site during cytokinesis. During polarized growth, Gef1
17 is required for bipolar Scd1 localization. Gef1 recruits Scd1 through the recruitment of the
18 scaffold Scd2; we propose this facilitates polarized cell growth at a second site. In turn, Scd1
19 restricts Gef1 localization to the division site and to the cell cortex, thus maintaining polarity. Our
20 results suggest that crosstalk between GEFs is a conserved mechanism that orchestrates
21 Cdc42 activation during complex processes.

22 INTRODUCTION

23 Growth and division are fundamental processes of all cells, and are essential for proper function
24 and proliferation. In most multicellular organisms, these two processes are precisely tuned to
25 control cell shape and function, to specify cell fate and differentiation, and to enable cell
26 adhesion and migration (Feigin and Muthuswamy, 2009; Godde et al., 2010; Halaoui and
27 McCaffrey, 2014; Lauffenburger and Horwitz, 1996). These processes are dependent on proper
28 cell polarization. Cell polarization relies on the ability of the cytoskeleton to establish unique
29 domains at the cell cortex to govern the local function and activity of specific proteins (Drubin
30 and Nelson, 1996; Nance and Zallen, 2011). The Rho family of small GTPases serves as the
31 primary regulator of the actin cytoskeleton, thereby controlling cell polarity and movement
32 (Ridley, 2006). Active Rho GTPases bind and activate downstream targets which regulate actin
33 cytoskeleton organization. GTPases are active when GTP-bound and inactive once they
34 hydrolyze GTP to GDP. Guanine nucleotide Exchange Factors (GEFs) activate GTPases by
35 promoting the binding of GTP, while GTPase Activating Proteins (GAPs) inactivate GTPases by
36 promoting GTP hydrolysis (Bos et al., 2007). Unraveling the regulation of these GEFs and
37 GAPs is at the crux of understanding how cell polarity is established, altered, and maintained.
38 One conserved member of the Rho family of small GTPases, Cdc42, is a master regulator of
39 polarized cell growth and membrane trafficking in eukaryotes (Estravis et al., 2012; Estravis et
40 al., 2011; Etienne-Manneville, 2004; Harris and Tepass, 2010; Johnson, 1999). In most
41 eukaryotes, Cdc42 is regulated by numerous GEFs and GAPs, which complicates our
42 understanding of GTPase regulation (Bos et al., 2007). In the fission yeast
43 *Schizosaccharomyces pombe*, Cdc42 is activated by two GEFs, Gef1 and Scd1 (Chang et al.,
44 1994; Coll et al., 2003). The presence of only two Cdc42 GEFs, and the well-documented
45 process of cell polarization, makes fission yeast an excellent model system to understand the
46 mechanistic details of cell shape establishment. Here we report that the two Cdc42 GEFs
47 regulate each other during both cytokinesis and polarized growth. This finding provides new
48 insights into the spatiotemporal regulation of Cdc42 during critical cellular events.

49 Cdc42, like other small GTPases, serves as a binary molecular switch and can respond to and
50 initiate multiple signaling pathways. In the budding yeast *Saccharomyces cerevisiae*, cells
51 develop only a single polarized site through a winner-take-all mechanism during bud emergence
52 (Iraoqui et al., 2003; Kozubowski et al., 2008; Slaughter et al., 2009a; Wedlich-Soldner et al.,
53 2004). However, a winner-take-all mechanism cannot explain how cells develop multiple
54 polarized sites that are frequently observed in higher eukaryotes. In contrast to budding yeast,
55 fission yeast grows in a bipolar manner, offering a model to understand how a cell regulates
56 polarized growth from multiple sites. In fission yeast, active Cdc42 displays anti-correlated
57 oscillations between the two ends (Das et al., 2012). These oscillations arise from both positive
58 and time-delayed negative feedback as well as competition between the two ends (Das et al.,
59 2012). This oscillatory pattern regulates cell dimensions and promotes bipolar growth in fission
60 yeast. Similar Cdc42 oscillations have been observed in natural killer cells during immunological
61 synapse formation (Carlin et al., 2011) and in budding yeast during bud emergence (Howell et
62 al., 2012). In plant cells, the ROP GTPases show oscillatory behavior during pollen tube growth
63 (Hwang et al., 2005). Furthermore, during migration in animal cells, the GTPases Rho, Rac, and
64 Cdc42 are sequentially activated to enable cell protrusion (Machacek et al., 2009). These

65 observations suggest that oscillatory behavior, which drives cell polarity, may be an intrinsic
66 property of GTPases that is likely conserved in most organisms (Das and Verde, 2013).

67 Most models of polarized growth propose the existence of Cdc42 positive feedback loops that
68 facilitate symmetry breaking through a winner-take-all mechanism (Bendezu et al., 2015;
69 Slaughter et al., 2009b). Our understanding of the molecular nature of these positive feedbacks
70 is primarily based on studies performed in budding yeast (Kozubowski et al., 2008; Slaughter et
71 al., 2009a; Slaughter et al., 2009b). In one model, Cdc42 activation via actin organization and
72 membrane trafficking amplifies its own localization to the polarized tip (Wedlich-Soldner et al.,
73 2004). Another model, based on studies in fission yeast, describe a positive feedback where
74 active Cdc42 captures inactive molecules to amplify the signal (Bendezu et al., 2015). In a
75 second model, a ternary complex consisting of the GEF Cdc24, the scaffold Bem1, and the Pak
76 kinase Cla4, amplifies Cdc42 activation at the cell's growth sites (Kozubowski et al., 2008). Both
77 models propose that active Cdc42 participates in the generation of the positive feedback. In
78 fission yeast, a similar ternary complex with the GEF Scd1, scaffold Scd2, and kinase Pak1 has
79 been reported (Endo et al., 2003). However, it is not clear how this complex mediates a positive
80 feedback loop during polarized growth.

81 To explain Cdc42 activation during polarized growth, it is important to first understand how
82 Cdc42 regulators function. Gef1 and Scd1 are partially redundant but exhibit unique phenotypes
83 when deleted (Chang et al., 1994; Coll et al., 2003), indicating that they may regulate Cdc42 in
84 distinct, but overlapping, manners. Scd1 oscillates between the two cell ends, much like active
85 Cdc42 (Das et al., 2012), and cells lacking *scd1* appear depolarized (Chang et al., 1994). Scd1
86 is also required for mating and contributes to Cdc42 dependent exploration of the cell cortex
87 (Bendezu and Martin, 2013). In contrast, *gef1* mutants become narrower and grow in a
88 monopolar, rather than a bipolar, manner (Coll et al., 2003). Furthermore, Cdc42 activity is
89 reduced at the new end in *gef1* mutants (Das et al., 2012). Gef1 shows sparse localization at
90 the cortex, making it difficult to determine whether it oscillates between cell ends (Das et al.,
91 2015). Understanding how two different Cdc42 GEFs yield distinct phenotypes will provide
92 valuable insights into Cdc42 regulation.

93 Investigations into the behaviors of Gef1 and Scd1 are complicated since these GEFs overlap at
94 sites of polarized growth during interphase. These GEFs also localize to the site of cell division
95 during cytokinesis (Wei et al., 2016). Cytokinesis, the final step in cell division, involves the
96 formation of an actomyosin ring that constricts, concurrent with cell wall (septum) deposition, to
97 enable membrane ingression and furrow formation (Pollard, 2010). The temporal localization
98 and function of the two GEFs are discernible during cytokinesis since they are recruited to the
99 division site in succession to activate Cdc42. During cytokinesis, Gef1 localizes first to the
100 actomyosin ring to activate Cdc42 and promote ring constriction (Wei et al., 2016). Scd1 then
101 localizes to the ingressing membrane and regulates septum formation (Wei et al., 2016). The
102 temporal difference between Gef1 and Scd1 localization at the division site allows us to
103 investigate the significance of multiple GEFs in Cdc42 regulation, which is unclear from studies
104 solely at the growing ends.

105 Using cytokinesis as a paradigm, here we identify a novel crosstalk between the GEFs, Gef1
106 and Scd1, that regulates Cdc42 activity during multiple cellular programs. We find that Gef1 and

107 Scd1 regulate each other during both cytokinesis and cell polarization. Our data indicates that
108 Gef1 promotes the localization of Scd1 to the division site. Contrary to previously proposed
109 models, constitutively active Cdc42 is not sufficient to rescue Scd1 localization in *gef1* mutants.
110 Instead, we find that Gef1 promotes the localization of the scaffold Scd2 to the division site
111 during cytokinesis, which then recruits Scd1. Next, we show that Scd1 promotes the removal of
112 Gef1 from the division site after completion of ring constriction. Furthermore, actin cables are
113 involved in Gef1 removal from the division site, suggesting that Scd1 promotes Gef1 removal
114 via an actin-mediated process. We extend these observations to the sites of polarized growth,
115 where we show that Gef1 promotes bipolar Scd1 and Scd2 localization; indeed, Gef1 is
116 necessary to recruit Scd1 to the non-dominant pole to initiate bipolar growth. In turn, Scd1 and
117 actin are necessary to prevent isotropic localization of Gef1 at the cell cortex during interphase,
118 thus maintaining polarity. By this manner of regulation, Cdc42 activation is promoted at the new
119 end of the cell with no prior growth history, but is restricted from random regions. Gef1 allows
120 growth initiation at the new end through the recruitment of Scd1, while Scd1 prevents ectopic
121 Gef1 localization. To the best of our knowledge, such crosstalk has not been reported to
122 function between GEFs of the same GTPase. The interplay between the Cdc42 GEFs operates
123 in the same manner during both cytokinesis and polarized growth, suggesting that this may be a
124 conserved feature of Cdc42 regulation.

125 RESULTS

126 **Gef1 promotes Scd1 recruitment to the division site**

127 We have reported that Gef1 localizes to the assembled actomyosin ring before Scd1 (Wei et al.,
128 2016). It is not clear why the cell recruits two distinct GEFs to the same site in a sequential
129 manner, given that they both activate Cdc42. Previous reports have demonstrated crosstalk
130 between GTPases via the modulation of their regulators (Guilluy et al., 2011). While there is no
131 report of GEFs of the same GTPase regulating each other, such an interaction could explain the
132 temporal relationship detected between Gef1 and Scd1 localization at the division site. Since
133 Scd1 arrives at the division site soon after Gef1, we posited that Gef1 may promote Scd1
134 localization. To test this, we examined whether Scd1 localization to actomyosin rings is Gef1-
135 dependent. Both Gef1 and Scd1 are low-abundance proteins and are not suitable for live cell
136 imaging over time. This complicates the investigation of these proteins in a temporal manner. To
137 overcome this limitation, we used the actomyosin ring as a temporal marker. The actomyosin
138 ring undergoes visibly distinct phases during cytokinesis: assembly, maturation, constriction,
139 and disassembly. We determined the timing of protein localization to the division site by
140 comparing it to the corresponding phase of the actomyosin ring. We have previously reported
141 that ring constriction is delayed in *gef1Δ* mutants (Wei et al., 2016). To eliminate any bias in
142 protein localization due to this delay, we only analyzed cells in which the rings had initiated
143 constriction. In *gef1Δ* mutants, the number of constricting rings that recruited Scd1-3xGFP
144 decreased to 15% from 96% in *gef1+* (Figure 1A,B, $p < 0.0001$). Furthermore, the *gef1Δ* cells
145 that managed to recruit Scd1-3xGFP did not do so as efficiently as *gef1+* cells, given the 15%
146 decrease in Scd1-3xGFP fluorescence intensity at the division site (Figure 1A,C, $p = 0.0098$).
147 Thus, Gef1 promotes Scd1 localization to the division site.

148 To better understand how Gef1 recruits Scd1 to the division site, we revisited the mechanism of
149 GEF recruitment in other systems. GEF recruitment to sites of Cdc42 activity occurs via positive
150 feedback, as reported in budding yeast (Butty et al., 2002; Kozubowski et al., 2008). In this
151 model, activation of Cdc42 leads to further recruitment of the scaffold Bem1, which then recruits
152 the GEF Cdc24 to the site of activity, thus helping to break symmetry and promote polarized
153 growth. A similar positive feedback may also exist in fission yeast (Das et al., 2012; Das and
154 Verde, 2013). We hypothesized that Gef1-activated Cdc42 acts as a seed for Scd1 recruitment
155 to the division site. To test this, we asked whether constitutive activation of Cdc42 could rescue
156 the Scd1 recruitment defect exhibited by *gef1Δ*. In order for this approach to work, the
157 constitutively active Cdc42 must localize to the division site. Localization of active Cdc42 is
158 visualized via the bio-probe CRIB-3xGFP that specifically binds GTP-Cdc42. Since our previous
159 work reported that Cdc42 activity is reduced at the division site in *gef1Δ* cells (Wei et al., 2016)
160 we validated this approach by first testing whether constitutively active Cdc42 restores CRIB-
161 3xGFP localization at the division site in *gef1Δ* cells. The empty control vector or the vector
162 expressing the constitutively active allele *cdc42G12V* under the control of the thiamine-
163 repressible *nmt41* promoter was integrated into the genome of *gef1+* and *gef1Δ* cells
164 expressing CRIB-3xGFP. Mild expression of *cdc42G12V* was sufficient to restore CRIB-3xGFP
165 intensity at the division site to physiological levels in *gef1Δ*, but not in *gef1Δ* with the control
166 vector (Figure 1D,F, $p < 0.0001$). Surprisingly, although expression of *cdc42G12V* was able to
167 restore Cdc42 activity at the division site in *gef1Δ* cells, it was unable to rescue Scd1-3xGFP

168 localization to the division site in *cdc42G12V gef1Δ* cells (Figure 1E,G). This demonstrates that
169 active Cdc42 alone is not sufficient to recruit Scd1, and that Gef1 is required for this process.

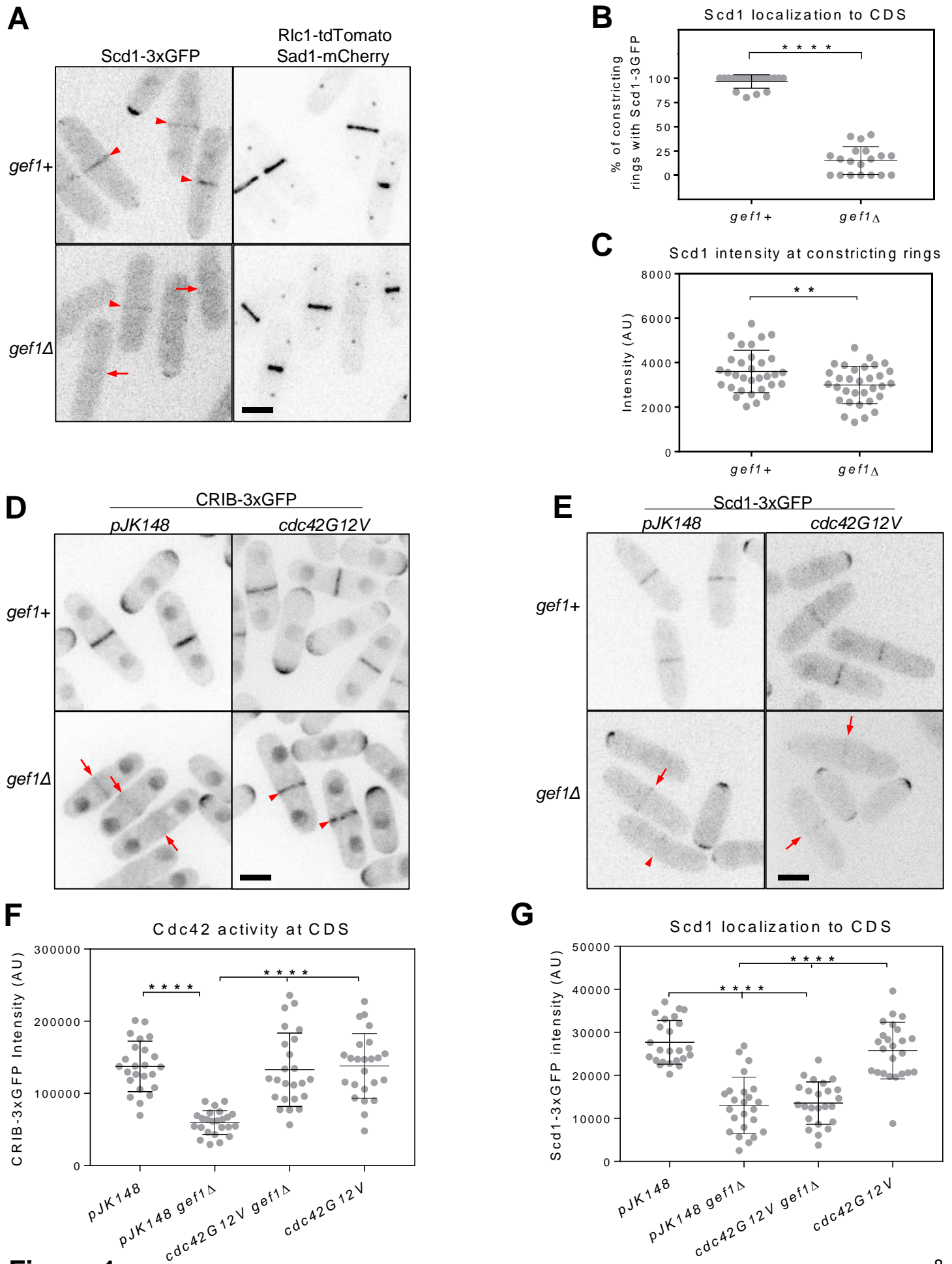


Figure 1

Figure 1: Gef1 promotes Scd1 localization to the division site. (A) Scd1-3xGFP localization in *gef1+* and *gef1Δ* cells expressing the ring and SPB markers Rlc1-tdTomato and Sad1-mCherry respectively. Arrowheads label cells with Scd1-3xGFP localized to the division site, while arrows mark cells with constricting rings that lack Scd1-3xGFP at the division site. **(B and C)** Quantification of Scd1-3xGFP localization and intensity in the indicated genotypes (**, $p < 0.01$). **(D)** CRIB-3xGFP, the active Cdc42 sensor, intensity at the division site in *gef1+* and *gef1Δ* cells transformed with the control vector *pJK148* or *cdc42G12V*. Arrows label cells with reduced Cdc42 activity at the division site and arrowheads indicate cells with increased Cdc42 activity. **(E)** Scd1-3xGFP localization at the division site in *gef1+* and *gef1Δ* cells transformed with the control vector *pJK148* or *cdc42G12V*. Arrows label cells with reduced Scd1-3xGFP at the division site. **(F and G)** Quantifications of *cdc42G12V*-mediated Cdc42 activity and Scd1 localization at the division site in the indicated genotypes (****, $p < 0.0001$). All data points are plotted in each graph, with black bars on top of data points that show the mean and standard deviation for each genotype. All images are inverted max projections. Scale bars = 5 μ m. Cell Division Site, CDS.

170 **Gef1 promotes Scd2 localization to the division site, which in turn recruits Scd1**

171 Next we asked if other members of the Cdc42 complex are involved in the recruitment of Scd1.
172 The Cdc42 ternary complex consists of the GEF Scd1, the scaffold protein Scd2, and the
173 downstream effector Pak1 kinase (Endo et al., 2003). Observations in budding yeast suggest
174 that the PAK kinase may mediate GEF recruitment (Kozubowski et al., 2008). Contrary to this
175 hypothesis, we find that Scd1-3xGFP intensity increases in the *nmt1 switch-off* mutant allele of
176 *pak1*, compared to *pak1+* cells (Figure S1). These findings support similar observations
177 reported in the hypomorphic temperature-sensitive *pak1* allele, *orb2-34* (Das et al., 2012).

178 Previous reports have shown that the scaffold Scd2 is required for Scd1 localization to the sites
179 of polarized growth (Kelly and Nurse, 2011). We hypothesized that Gef1 recruits Scd1 to the
180 division site through the scaffold Scd2. Thus, we examined whether Scd2-GFP localization to
181 the division site is Gef1-dependent. *gef1Δ* cells displayed a significant decrease in the number
182 of assembled rings that recruited Scd2-GFP compared to *gef1+*. In *gef1Δ* mutants, the number
183 of rings that recruited Scd2-GFP prior to ring constriction decreased to 8% compared to 88% in
184 *gef1+*, indicating a delay in Scd2 recruitment (Figure 2A,B, $p>0.0001$). Although *gef1Δ* cells
185 managed to recruit Scd2 to the division site once ring constriction began, the fluorescence
186 intensity of Scd2-GFP at the division site was reduced by 61% compared to *gef1+* cells (Figure
187 2A,C, $p>0.0001$, Fig. S2). Gef1 thus promotes Scd2 localization to the division site.

188 Since previous work indicated that Scd1 and Scd2 require each other for their localization (Kelly
189 and Nurse, 2011), it is possible that a decrease in Scd2 at the division site observed in *gef1*
190 mutants is due to a decrease in Scd1 at this site. However, contrary to previous findings, we
191 observed that Scd2-GFP localization at the division site is not impaired in *scd1Δ* cells (Figure
192 2E). In contrast, Scd1-3xGFP localization is completely abolished at the division site in *scd2Δ*
193 cells (Figure 2E). We find that while Scd1 requires Scd2 for its localization to the division site,
194 Scd2 localization is independent of Scd1. Altogether, this reveals that Gef1 promotes Scd2
195 localization to the division site, which is required for Scd1 localization. To further validate these
196 findings, we examined the temporal localization of Gef1, Scd1, and Scd2 to the division site. A
197 well-established temporal marker for cells in cytokinesis is the distance between the spindle
198 pole bodies. The spindle pole body distance increases as mitosis progresses until the cell
199 reaches anaphase B (Nabeshima et al., 1998), at which time the actomyosin ring starts to
200 constrict (Wu et al., 2003). The distance between the two spindle pole bodies can thus act as an
201 internal clock that helps to time the recruitment of other proteins. We acquired numerous still
202 images and calculated the distance between the spindle pole bodies, marked by Sad1-mCherry,
203 during anaphase A or anaphase B. We report the spindle pole body distance at which Gef1-
204 mNG (monomeric NeonGreen), Scd1-3xGFP, and Scd2-GFP signals are visible at the non-
205 constricting actomyosin ring (Figure 2F). Next, we calculated the mean spindle pole body
206 distance of the first 50th percentile of our data. The protein that localizes earliest to the
207 actomyosin ring during mitosis will display the smallest mean spindle pole body distance. We
208 find that Gef1-mNG localized to the actomyosin ring with a mean spindle pole body distance of
209 3.2 μ m, Scd2-GFP with a mean distance of 4.1 μ m and Scd1-3xGFP with a mean distance of
210 5.1 μ m (Figure 2G). This demonstrates that Gef1-mNG is recruited to the actomyosin ring first,
211 followed by Scd2-GFP, and finally Scd1-3xGFP. The sequence in which these proteins localize

212 to the division site agrees with our earlier results, which show that Gef1 recruits Scd1 indirectly
213 through Scd2.

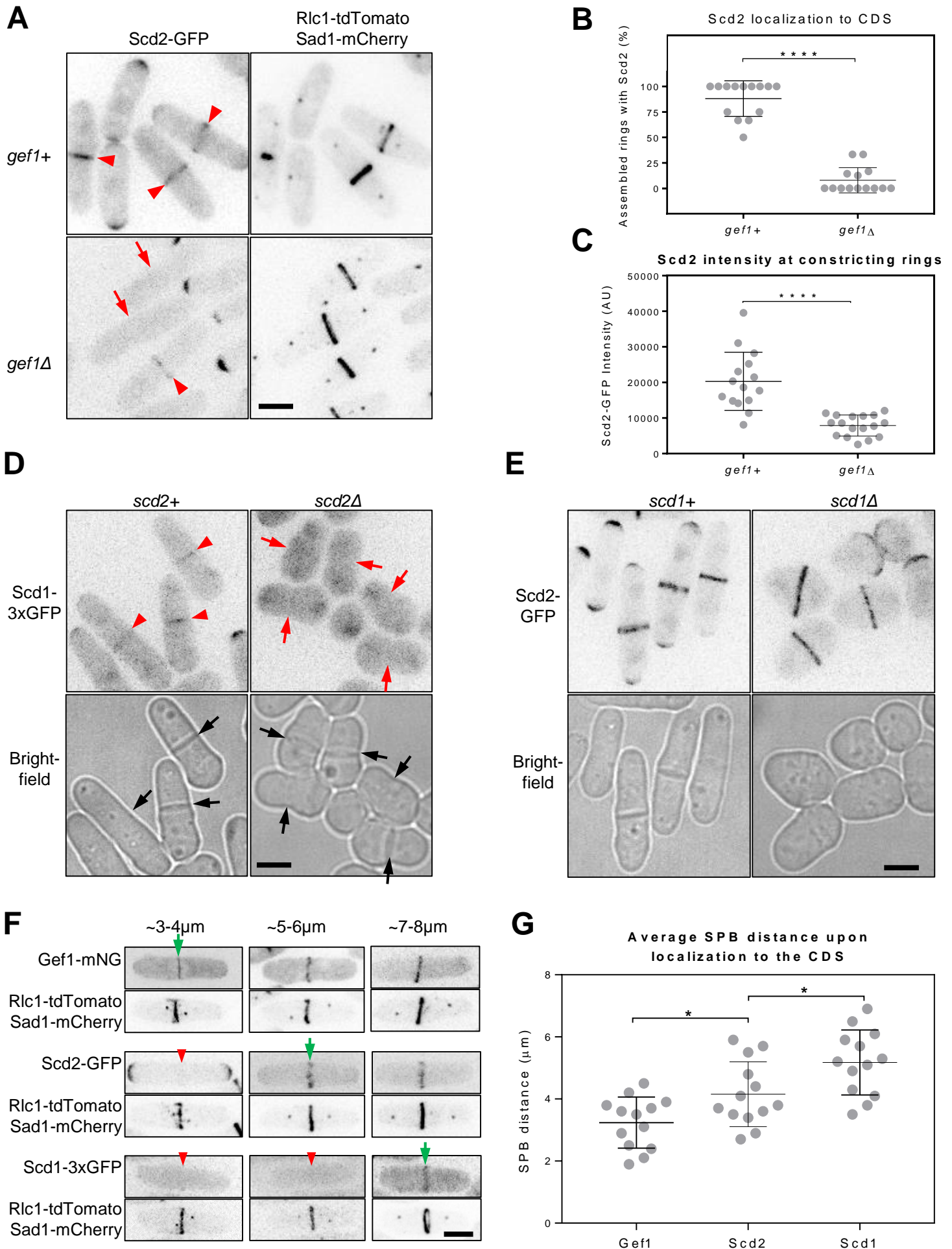


Figure 2

Figure 2: Gef1 promotes Scd1 localization to the division site via recruitment of Scd2. (A) Scd2 localization in *gef1+* and *gef1Δ* cells expressing the ring and SPB markers Rlc1-tdTomato and Sad1-mCherry. Arrowheads label cells with Scd2-GFP localized constricting rings, while arrows mark cells with assembled rings that lack Scd2-GFP at the division site. **(B and C)** Quantification of Scd2-GFP localization and intensity in the indicated genotypes (****, $p < 0.0001$). **(D)** Scd1-3xGFP localization in *scd2+* and *scd2Δ* cells. Division site marked by black arrows in the bright field images. Scd1-3xGFP localization to the division site indicated by red arrowheads. Red arrows show absence of Scd1-3xGFP at the division site. **(E)** Scd2-GFP localization to the division site in *scd1+* and *scd1Δ* cells. **(F)** Representative images showing the localizations of Gef1-mNG, Scd2-GFP, and Scd1-3GFP (top panels) as a function of spindle pole body distance (bottom panels). The range of SPB distance is listed for each column. Green arrows indicate the earliest time point at which signal is visible. Red arrowheads indicate time points prior to localization. **(G)** Quantification of Gef1, Scd2, and Scd1 localization to the division site in a temporal manner, showing the means of the distance between spindle poles of the first 50th percentile of early anaphase cells at which signal first appears (*, $p < 0.05$). All data points are plotted in each graph, with black bars on top of data points that show the mean and standard deviation for each genotype. All images are inverted max projections with the exception of bright field. Scale bars = 5 μ m. Cell Division Site, CDS.

214 **Scd1 promotes Gef1 removal from the division site at the end of ring constriction**

215 Once the actomyosin ring constricts, Gef1 constricts with it and is lost from the division site
216 when the ring disassembles (Wei et al., 2016). At this stage, Scd1 is still localized to the
217 membrane barrier. Since our data show that Gef1 promotes Scd1 localization, we asked if Scd1
218 mediates Gef1 localization to the division site. We did not detect any aberrant Gef1 behavior
219 during early cytokinetic events in cells lacking *scd1*. However, at the end of ring constriction, we
220 observed prolonged Gef1 localization in *scd1* mutants. In *scd1+* cells, Gef1 localizes to the
221 membrane adjacent to the ring throughout constriction. In cells that have completed constriction,
222 Gef1 is lost as the ring disassembles (Figure 3A). In *scd1Δ* mutants, after completion of ring
223 constriction and disassembly, Gef1 remains at the membrane that was adjacent to the ring. In
224 70% of *scd1Δ* cells, post-ring-disassembly, Gef1-mNG persists at the newly formed membrane
225 barrier, as confirmed by the absence of Rlc1-tdTomato (Figure 3A,B). Similar Gef1-mNG
226 localization was observed in only 20% of *scd1+* cells (Figure 3B, $p < 0.0001$).

227 To understand how Scd1 mediates Gef1 removal from the membrane barrier after constriction,
228 we analyzed the phenotype of *scd1Δ* mutants. We find that the actin cytoskeleton is disrupted in
229 *scd1Δ* cells, as observed by Alexa Fluor Phalloidin staining. *scd1Δ* cells accumulate actin
230 patches and have fewer and more disorganized actin cables (Figure S3). Therefore, we
231 examined the role of actin in Gef1 removal after ring constriction. We treated the cells with
232 Latrunculin A (LatA) to disrupt the actin cytoskeleton. In LatA treated cells that were fully
233 septated following completion of constriction, we observed persistent Gef1 localization at the
234 division site. Gef1-mNG persists on both sides of the septum barrier in 40% of cells treated with
235 LatA, but not in mock DMSO-treated cells (Figure 3C). Cells undergoing ring constriction and
236 septum formation display actin cables as well as Arp2/3-complex-dependent patches at the
237 division site (Coffman et al., 2013; Gachet and Hyams, 2005; Huang et al., 2012; Wang et al.,
238 2016). LatA treatment removes all types of filamentous actin structures (Spector et al., 1983).
239 To determine which actin-mediated process regulates Gef1 removal, we treated cells with
240 CK666 to block only Arp2/3-mediated branched actin filaments (Sun et al., 2011). In these cells,
241 Gef1-mNG removal was unhindered, as in DMSO-treated control cells, or localized to random
242 sites along the cortex, but did not persist at the division site (Figure 3C). This reveals that Gef1
243 removal at the end of ring constriction is independent of branched actin. We next examined the
244 role of filamentous actin cables in the removal of Gef1 from the membrane barrier. Cdc42
245 activates the formin For3 to promote actin polymerization and cable formation (Feierbach and
246 Chang, 2001; Martin et al., 2007). We investigated whether Gef1 removal from the membrane
247 barrier is *for3*-dependent. We find that in *for3Δ*, Gef1-3xYFP lingers at the membrane adjacent
248 to the ring after completion of constriction, just as in *scd1Δ* (Figure 3E). To determine whether
249 Gef1 removal by Scd1 and by actin operates in the same or parallel pathways, we treated
250 *scd1+* and *scd1Δ* cells expressing Gef1-mNG with LatA. We find that in cells treated with
251 DMSO, Gef1-mNG persists in 20% of septated *scd1+* cells and in 63% of septated *scd1Δ* cells.
252 In cells treated with LatA, Gef1-mNG persists in 40% of septated *scd1+* cells and in 61% of
253 septated *scd1Δ* cells (Figure 3D). The extent of Gef1 persistence in *scd1Δ* cells does not
254 increase with the addition of LatA, indicating that Scd1 is epistatic to actin-mediated removal
255 (Figure 3D). Together, these data suggest that Scd1 removes Gef1 from the division site after
256 ring disassembly through an actin-mediated process involving the formin For3.

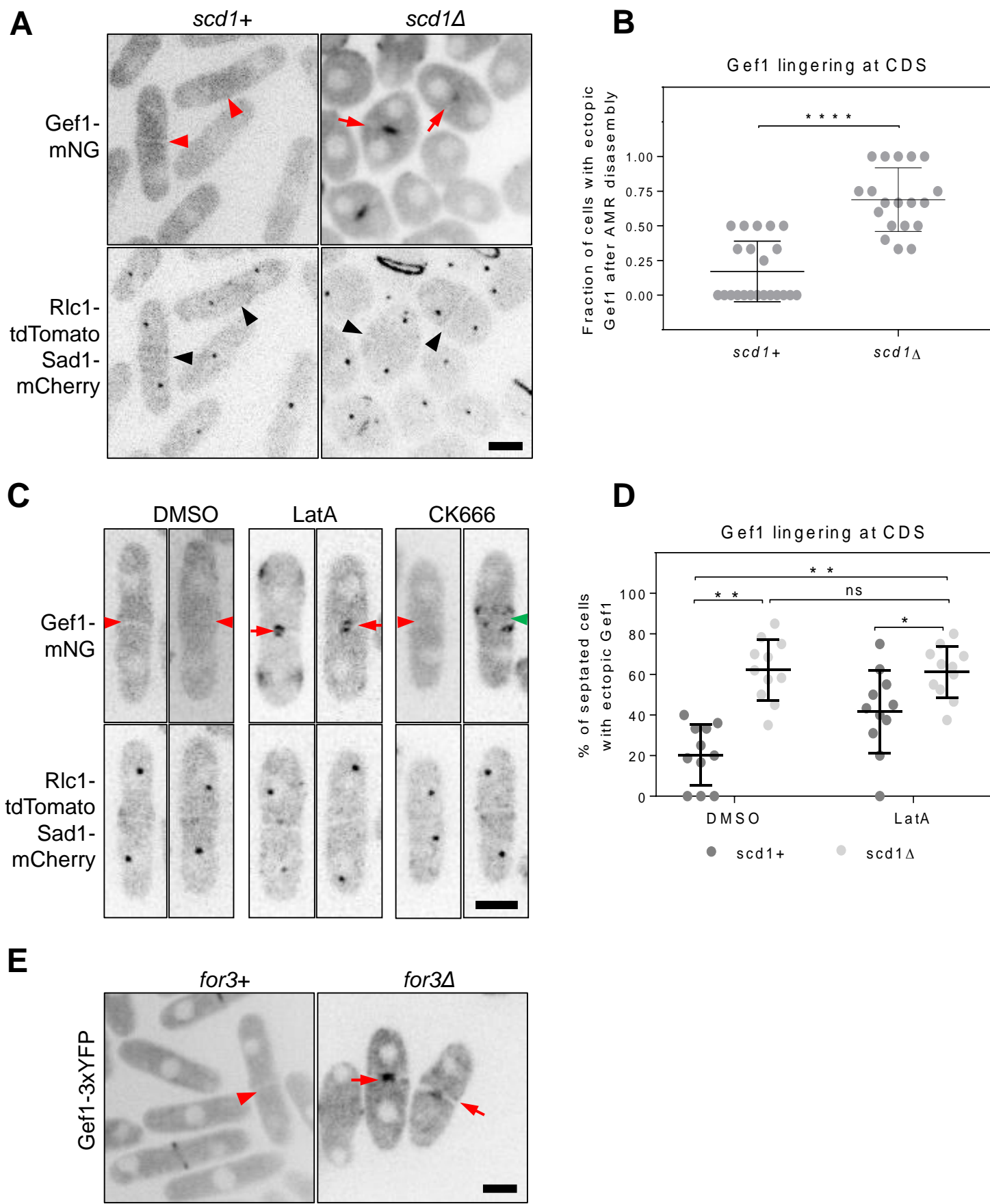


Figure 3

Figure 3: Scd1 and actin promote Gef1 removal from the division site after ring constriction. (A)

Gef1-mNG localization to the division site after ring disassembly in *scd1+* and *scd1Δ* cells expressing the ring and SPB markers Rlc1-tdTomato and Sad1-mCherry. Black arrowheads mark the membrane barrier in cells post-ring disassembly. Red arrowheads mark cells post-ring disassembly that lack Gef1-mNG at the membrane barrier. Red arrows mark cells with Gef1-mNG localized to the membrane barrier post-ring assembly. **(B)** Quantification of Gef1 lingering at the division site in *scd1+* and *scd1Δ* cells (****, $p < 0.0001$). **(C)** Gef1-mNG localization in septated cells expressing the ring and SPB markers Rlc1-tdTomato and Sad1-mCherry, treated with either DMSO, 10 μ M LatA, or 100 μ M CK666. Red arrowheads mark cells post-ring disassembly that lack Gef1-mNG at the membrane barrier. Red arrows indicate cells with Gef1-mNG localized to the membrane barrier post-ring assembly. Green arrowheads indicate cells with Gef1-mNG localized to the cortex orthogonal to the membrane barrier. **(D)** Quantification of Gef1 lingering at the division site in septated *scd1+* and *scd1Δ* cells treated with 10 μ M LatA or DMSO (*, $p < 0.05$. **, $p < 0.01$). **(E)** Gef1-3xYFP localization in *for3+* and *for3Δ* cells. Red arrowheads mark cells post-ring disassembly that lack Gef1-3xYFP at the membrane barrier. Red arrows mark cells with Gef1-3xYFP localized to the membrane barrier post-ring assembly. All data points are plotted in each graph, with black bars on top of data points that show the mean and standard deviation for each genotype. All images are inverted max projections. Scale bars = 5 μ m. Cell Division Site, CDS.

257 **Gef1 is required for bipolar Scd1 localization**

258 Our data reveal an interesting interplay between the two Cdc42 GEFs in which they regulate
259 each other's localization during cytokinesis. We inquired whether this novel interaction is
260 intrinsic to the regulation of Cdc42 in other cellular processes. Cdc42 and its GEFs play a
261 supporting role in cytokinesis, but are central players in the regulation of polarized growth. Thus,
262 we asked whether a similar interaction occurs at sites of polarized growth. Gef1 promotes
263 bipolar growth in fission yeast (Coll et al., 2003; Das et al., 2012). Cells lacking *gef1* show
264 increased monopolarity, with polarized growth only occurring at the old end. In fission yeast
265 cells, Scd1 localizes to sites of polarized growth (Das et al., 2009; Kelly and Nurse, 2011);
266 accordingly, cells in early G2 phase display Scd1 localization at the old end. Cells in late G2,
267 which have undergone new-end-take-off (NETO), grow in a bipolar manner and display Scd1
268 localization at both the old and new end of the cell. We inquired whether Gef1 promotes Scd1
269 localization at sites of polarized growth. Scd1, like active Cdc42, undergoes oscillations
270 between the two competing ends (Das et al., 2012); thus, a cell undergoing bipolar growth does
271 not always display bipolar Scd1 localization. We found that Scd1-3xGFP levels at the old end
272 were comparable in *gef1+* and *gef1Δ* cells (Figure S4). However, *gef1Δ* cells exhibited fewer
273 new ends with Scd1-3xGFP; bipolar Scd1-3xGFP was observed in 30% of interphase *gef1+*
274 cells, but only in 14% of *gef1Δ* cells (Figure 4A,B, $p=0.0004$). Similarly, we also observed a
275 decrease in bipolar Scd2 in cells lacking *gef1*; 70% of *gef1+* cells displayed bipolar Scd2-GFP
276 localization, but this was reduced to 30% in *gef1Δ* cells (Figure 4A,B, $p<0.0001$). Similar to what
277 we find at the site of cell division, Scd2 is required for Scd1 localization to sites of polarized
278 growth, but Scd2 localization is independent of Scd1 (Figure 4F). In *scd1Δ* mutants, Scd2-GFP
279 signal was observed either at cell ends or ectopically at the cell cortex. In contrast, *scd2Δ*
280 mutants failed to localize Scd1-3xGFP to the cell cortex, forcing its accumulation within the
281 nucleus or cytoplasm. Thus, Gef1 promotes Scd2 localization, which in turn recruits Scd1 to
282 sites of polarized growth.

283 Next, we tested whether active Cdc42 can restore bipolar Scd1 localization in *gef1Δ* cells. To
284 examine this, we first checked to see whether expression of constitutively active Cdc42 results
285 in bipolar localization of active Cdc42, as indicated by CRIB-3xGFP localization. Low-level
286 expression of *cdc24G12V* was sufficient to restore bipolar CRIB-3xGFP localization in *gef1Δ*,
287 compared to the empty-vector-containing *gef1Δ* mutants (Figure 4B,E, $p<0.0001$). We observed
288 bipolar CRIB-3xGFP in 75% of *gef1+* cells transformed with the empty vector and in 93% of
289 cells expressing *cdc14G12V*. In *gef1Δ* mutants transformed with the empty vector, we observed
290 bipolar CRIB-3xGFP in only 50% of cells. In contrast, in *gef1Δ* mutants, low levels of
291 *cdc42G12V* expression restored bipolar CRIB-3xGFP in 92% of cells. Next we investigated
292 whether *cdc42G12V* restored bipolar Scd1-3xGFP localization in *gef1Δ* cells. Expression of
293 *cdc42G12V* was unable to restore bipolar Scd1-3xGFP localization to the cell ends in *gef1Δ*
294 mutants, just as it did not rescue Scd1 localization to the division site (Figure 3C). We observed
295 bipolar Scd1-3xGFP in 28% of *gef1+* cells transformed with the empty vector, and in 31% of
296 cells expressing *cdc42G12V*. In *gef1Δ* mutants transformed with the empty vector, we observed
297 bipolar Scd1-3xGFP in only 12.5% of cells. Further, in *gef1Δ* mutants expressing low levels of
298 *cdc42G12V*, bipolar Scd1-3xGFP remained in only 12.6% of cells (Figure 4C,E). This indicates
299 that *cdc42G12V*, while sufficient to restore bipolar growth, cannot promote bipolar Scd1

300 localization in the absence of *gef1*. This further demonstrates that Gef1 is required for bipolar
301 Scd1 localization.

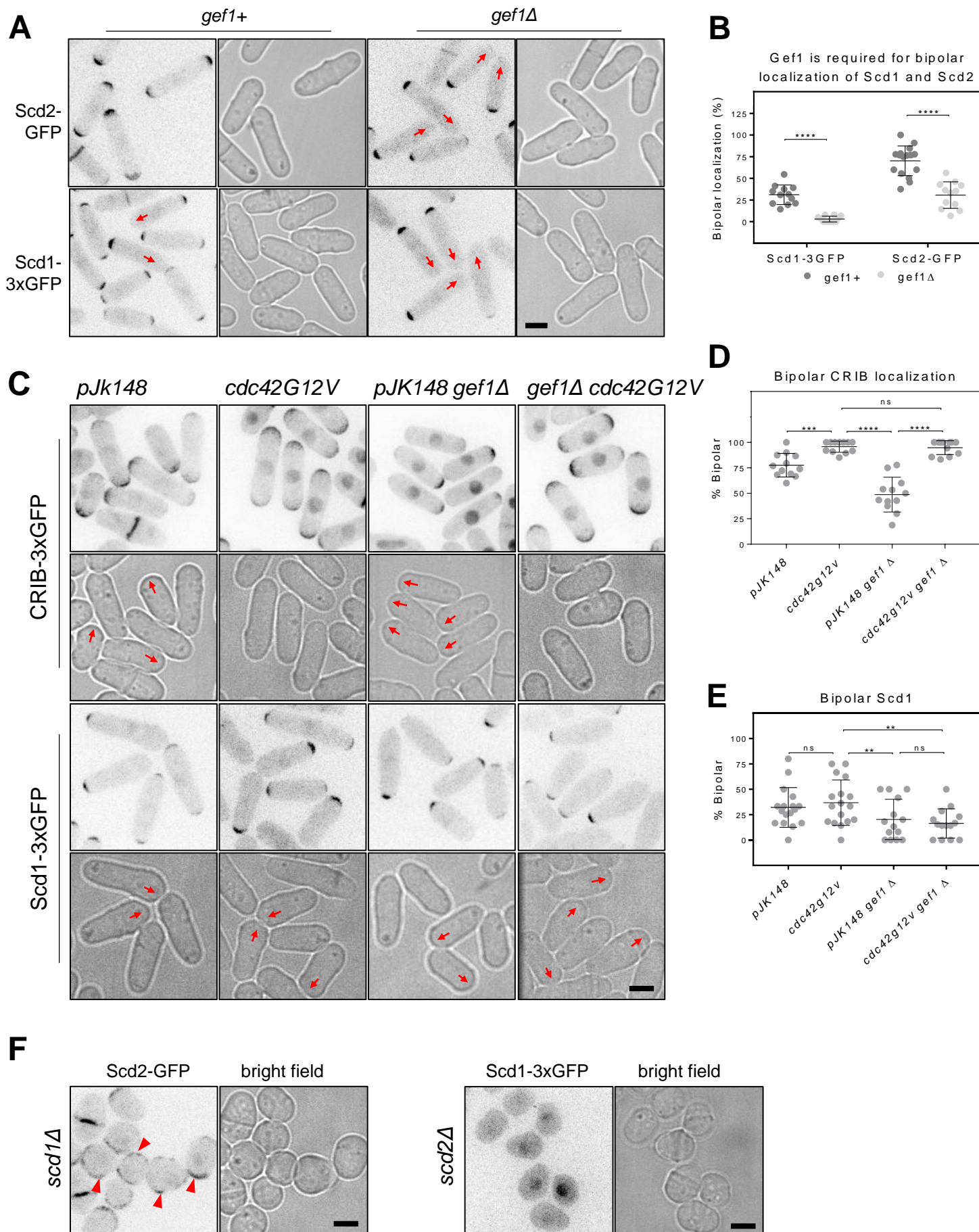


Figure 4

Figure 4: Gef1 promotes Scd1 localization to the new end. (A) Scd2-GFP (top panel) and Scd1-3xGFP (bottom panel) localization to the sites of polarized growth in *gef1+* and *gef1Δ* cells. Red arrows indicate the new ends of monopolar cells that do not recruit Scd2-GFP or Scd1-3xGFP. **(B)** Quantifications of bipolar Scd1-3xGFP and Scd2-GFP localization in the indicated genotypes (***, $p < 0.001$, ****, $p < 0.0001$). **(C)** CRIB-3xGFP and Scd1-3xGFP localization at cell tips, and restoration of bipolar growth in *gef1+* and *gef1Δ* cells transformed with the control vector *pJK148* or *cdc42G12V*. Red arrows indicate the new end of monopolar cells. **(D and E)** Quantification of the percent of cells that exhibit bipolar CRIB-3xGFP and Scd1-3xGFP localization at cell tips in the indicated genotypes (**, $p < 0.01$). **(F)** Scd2-GFP and Scd1-3xGFP localization to the cortex in *scd1Δ* and *scd2Δ* cells, respectively. Red arrows indicate cells with Scd2-GFP localized to the cell cortex. All data points are plotted in each graph, with black bars on top of data points that show the mean and standard deviation for each genotype. All images are inverted max projections with the exception of bright field unless specified. Scale bars = 5 μ m.

302 **Gef1 establishes polarized growth at the new end**

303 Our data suggest that Gef1 promotes bipolar growth in fission yeast by enabling bipolar Scd1
304 localization. However, previous reports have shown that while *gef1Δ* mutants are mainly
305 monopolar, about 40% of interphase cells show bipolar growth (Figure 5B) (Coll et al., 2003;
306 Das et al., 2012; Das et al., 2015). If Gef1 is required for Scd1 localization to the new end, how
307 does bipolar growth occur in some *gef1Δ* cells? To address this, we investigated the nature of
308 bipolar growth in *gef1Δ* mutants. Fission yeast cells have an old end that existed in the previous
309 generation and a new end that was formed as a result of cell division. The old end initiates
310 growth immediately after completion of division and cell separation. As the cell grows, it
311 eventually initiates growth at the new end, resulting in bipolar growth (Figure 5A) (Mitchison and
312 Nurse, 1985). The two ends in fission yeast compete for active Cdc42, and initially the old end
313 wins this competition (Das et al., 2012). The old end can thus be said to be dominant over the
314 new end in a newborn cell, and always initiates growth first. The new end must overcome the
315 old end's dominance in order to initiate its own growth.

316 We find that 68% of monopolar *gef1Δ* mutant cells exhibit a growth pattern in which one
317 daughter cell is monopolar and the other daughter cell is prematurely bipolar (Figures 5B and
318 S5). In monopolar *gef1Δ* cells, growth predominantly occurs at the old end, which grew in the
319 previous generation (Figures 5B and S5). In these monopolar cells, the new end frequently fails
320 to grow since it cannot overcome the old end's dominance. The daughter cell that inherits its
321 parent cell's non-growing end typically displays precocious bipolar growth, indicating that these
322 cells do not contain a dominant end. Our data suggest that for a cell end to be dominant it
323 needs to have grown in the previous generation. These results indicate that the new ends of
324 *gef1* cells are not well-equipped to overcome old end dominance. Indeed, we find that in *gef1+*
325 cells, 97% of daughter cells derived from a growing end display a normal growth pattern in
326 which new end take-off occurs only after the old end initiates growth (Figure 5C). In *gef1Δ* cells,
327 only 9% of daughter cells derived from a growing end display the same pattern; instead, 81% of
328 daughter cells derived from a growing end failed to initiate growth at their new end and were
329 thus monopolar (Figure 5C). These observations show that Gef1 enables the new end to
330 overcome old end dominance to promote bipolar growth.

331 Taken together, our findings demonstrate that Gef1 helps promote bipolar growth by enabling
332 Scd1 localization to the new end. This is further supported by our previous observation that the
333 hyperactive *gef1* mutant allele *gef1S112A* shows premature bipolar growth (Das et al., 2015).
334 Gef1 sparsely localizes to cell ends and instead remains mainly cytoplasmic. Gef1 is
335 phosphorylated by the NDR kinase Orb6 (Das et al., 2009), resulting in a 14-3-3 binding site
336 (Das et al., 2015). Interaction with a 14-3-3 protein sequesters Gef1 to the cytoplasm and away
337 from the cortex. The *gef1S112A* mutation eliminates the Orb6 phosphorylation site, thus
338 enabling excessive Gef1S112A localization to both cell ends, where it activates Cdc42 to
339 promote premature bipolar growth (Das et al., 2015). Consistent with these findings, we report
340 that Scd1 is significantly more bipolar in *gef1S112A* mutants. 53% of *gef1S112A* cells exhibit
341 Scd1-3xGFP localization at both ends, compared to 32% in *gef1+* cells (Figure 5D,E,
342 $p < 0.0001$). These findings support the hypothesis that Gef1 overcomes old end dominance by
343 recruiting Scd1 to the new end to establish a nascent growth site.

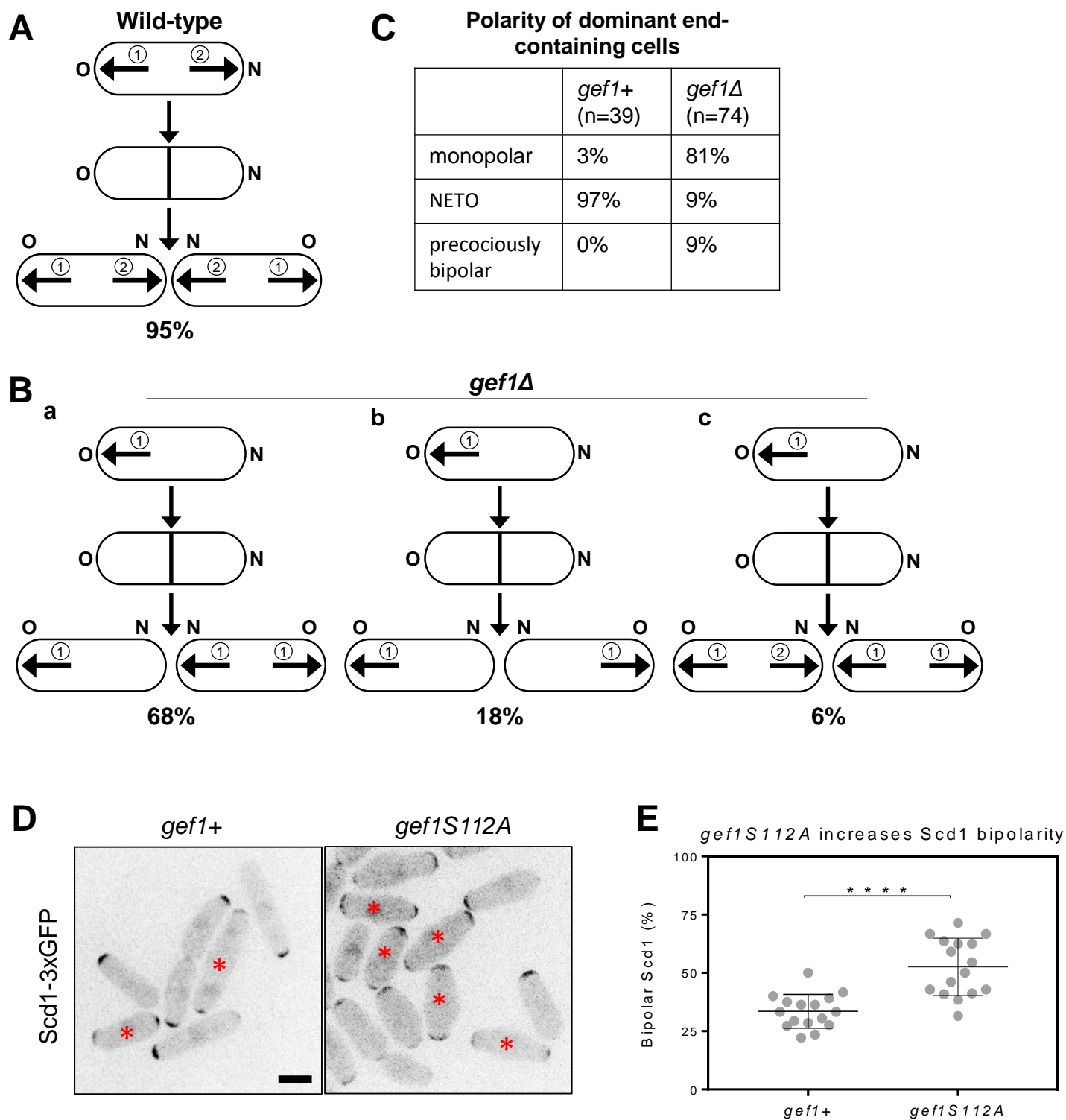


Figure 5

Figure 5: Gef1 promotes bipolar growth via new-end-take-off . (A) Wild-type cells predominately display old end growth followed by a delayed onset of new-end growth. (B) **i.** In *gef1Δ*, 68% of monopolar cells yield a monopolar cell from the end that grew in the previous generation and a bipolar cell from the end that failed to grow in the previous generation. **ii.** 18% of monopolar cells yield two monopolar cells. **iii.** 6% of monopolar cells yield two monopolar cells. Circled numbers describe the order of growth. Arrows correspond to direction of growth. (C) Quantification of the fate of *gef1+* and *gef1Δ* cells with a dominant end. (D) Localization of Scd1-3xGFP to the cell poles in *gef1+* and *gef1S112A* cells. Asterisks indicate cells with bipolar Scd1-3xGFP localization. (E) Quantification of the percent of cells that exhibit bipolar Scd1-3xGFP localization at cell ends in the indicated genotypes (****, $p < 0.0001$). Scale bar = 5 μ m.

344 **Scd1 is required to restrict Gef1 localization to the cell ends**

345 Next, we asked whether Scd1 and actin similarly regulate Gef1 at sites of polarized growth.
346 Cells lacking *scd1* are round, and under a cell cycle arrest, these cells show polarized growth
347 with increased cell width (Chang et al., 1994; Kelly and Nurse, 2011). We find that active Cdc42
348 appears depolarized in *scd1Δ* mutants during interphase. While CRIB-3xGFP remains restricted
349 to the ends in *scd1+* cells, in *scd1Δ* mutants its localization appears depolarized with random
350 patches all over the cortex (Figure 6Bi, iii). We find that in *scd1+* cells, Gef1-mNG displayed
351 sparse but polarized localization at cell ends (Figure 6Ai). In *scd1Δ* mutants, Gef1-mNG showed
352 better cortical localization when compared to *scd1+* cells (Fig. 6Aiii). Further, Gef1-mNG
353 showed depolarized cortical localization in *scd1Δ* mutants with random patches all over the
354 cortex. This indicates that Scd1 is required to restrict Gef1 localization to the cell ends, thus
355 maintaining polarized growth.

356 Since we find that actin plays a role in the removal of Gef1 from the division site (Figure 3C), we
357 ask whether actin also regulates Gef1 localization at sites of polarized growth. We treated cells
358 expressing Gef1-mNG with DMSO or LatA. Gef1-mNG localizes to the ends of control cells
359 treated with DMSO. Upon LatA treatment, Gef1-mNG localizes to ectopic patches at the cortex
360 (Figure 6Ai, ii). Next, we analyzed Gef1-mNG localization in LatA-treated *scd1Δ* mutants. In
361 *scd1Δ* mutants treated with either DMSO or LatA, we find that Gef1-mNG localizes to broad
362 patches along the cortex (Figure 6Aiii, iv). To determine if ectopic Gef1 at the cortex in *scd1Δ*
363 mutants or LatA-treatment of cells results in ectopic Cdc42 activation, we analyzed CRIB-
364 3xGFP localization in these cells. We find that in cells treated with LatA, CRIB-3xGFP localizes
365 randomly to the cortex, signifying ectopic Cdc42 activation, similar to previous reports
366 (Mutavchiev et al., 2016). In mock DMSO-treated control cells, CRIB-3xGFP forms caps at the
367 growing ends (Figure 6Bi). Upon treatment with LatA, CRIB-3xGFP localizes ectopically to
368 diffuse cortical patches (Figure 6Bii). Similarly, CRIB-3xGFP localization appears as diffuse
369 cortical patches in *scd1Δ* mutants (Figure 6Biii). If ectopic Cdc42 activation in LatA-treated cells
370 occurs due to ectopic Gef1 localization, then loss of *gef1* should restore polarized Cdc42
371 activation in these cells. Indeed, CRIB-3xGFP remains polarized upon LatA treatment in *gef1Δ*
372 mutants (Figure 6Bvi). In *scd1Δ* mutants, CRIB-3xGFP localization appears ectopic in cells
373 treated with either DMSO or LatA (Figure 6iii, iv). Together, these data demonstrate that Scd1
374 and actin are required to prevent ectopic Gef1 localization and Cdc42 activation to maintain
375 proper cell shape.

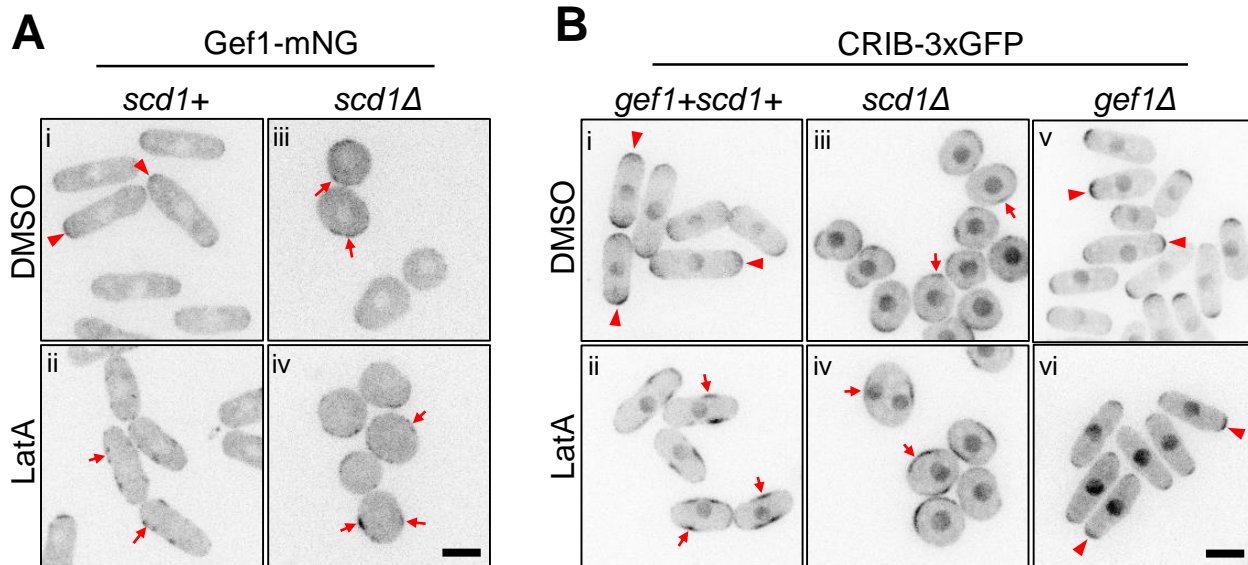


Figure 6: Scd1 and actin prevent ectopic Gef1 localization to promote polarized growth. (A) Gef1-mNG localization in *gef1+* and *gef1Δ* cells treated with DMSO (top panel) or 10μM LatA (bottom panel). **(B)** CRIB-3xGFP localization in *gef1+* and *gef1Δ* cells treated with DMSO (top panel) or 10μM LatA (bottom panel). Arrowheads indicate cells with CRIB-3xGFP or Gef1-mNG localized to regions of polarized growth. Arrows indicate cells with CRIB-3xGFP or Gef1-mNG localized to non-polarized regions on the cell cortex. All images are inverted max projections of the medial 4-7 cell slices. Scale bar = 5μm.

376 **DISCUSSION**

377 While Cdc42 is a major regulator of polarized cell growth, its regulation is not well understood,
378 largely due to the presence of multiple activators and inhibitors that often function in a
379 redundant manner. In fission yeast, Cdc42 is activated by only two GEFs, Gef1 and Scd1
380 (Chang et al., 1994; Coll et al., 2003). While these GEFs are partially redundant (Coll et al.,
381 2003; Hirota et al., 2003), they display distinct phenotypes and it is unclear why the cell requires
382 two Cdc42 GEFs. We have recently shown that Gef1 and Scd1 localize sequentially to the
383 division site to activate Cdc42 during cytokinesis (Wei et al., 2016). Here we take advantage of
384 the temporal difference between Gef1 and Scd1 localization at the division site to determine the
385 significance of these two GEFs in Cdc42 regulation. We uncover a novel interplay between the
386 Cdc42 GEFs that functions in both cytokinesis and polarized cell growth (Figure 7A). Given the
387 conserved nature of Cdc42 and its regulators, we posit that this interplay between the GEFs is a
388 common feature of Cdc42 regulation.

389

390 **Crosstalk between Gef1 and Scd1 during cytokinesis**

391 We have previously reported that Gef1 recruitment precedes Scd1 localization to the division
392 site (Wei et al., 2016). Given that Scd1 appears to be the primary Cdc42 GEF, we asked
393 whether the role of Gef1 is to recruit Scd1. Indeed, we report that Scd1 localizes to the division
394 site in a Gef1-dependent manner (Figure 7B). We report that Scd1 is recruited by its scaffold
395 Scd2, which is in turn recruited by Gef1 (Figure 7A,B). Furthermore, we show that while Scd1
396 localization is dependent on Scd2, the reciprocal is not true. Unlike the cell ends, the division
397 site has no prior history of Cdc42 activation or Scd1 localization. It is possible that the division
398 site, lacking a prior history of Cdc42 activation, requires Gef1 to recruit Scd1 to this nascent site.

399 Mis-regulation of Cdc42 has been reported to result in cytokinesis failure in many organisms.
400 Specifically, failure to inactivate Cdc42 leads to failed cell abscission in budding yeast and HeLa
401 cells, and prevents cellularization in *Drosophila* embryos (Atkins et al., 2013; Crawford et al.,
402 1998; Dutartre et al., 1996; Onishi et al., 2013). The mechanism by which Cdc42 is inactivated
403 prior to cell abscission has not been investigated in fission yeast. Gef1 localization to the
404 division site is lost after ring constriction (Wei et al., 2016). Here, we show that Scd1 promotes
405 the clearance of Gef1 from the division site after ring disassembly (Figure 7A). This suggests
406 that Scd1 ensures that Gef1 does not persist at the division site in the final stages of
407 cytokinesis, preventing inappropriate Cdc42 activation. Our data also show that Gef1 removal
408 depends on the presence of actin cables and the formin For3 (Figure 7A). Actin cytoskeleton
409 organization is primarily regulated by Cdc42 (Sit and Manser, 2011). We find that *scd1Δ*
410 mutants show depolarized actin cables and patches likely due to mis-regulation of Cdc42. We
411 posit that Scd1-dependent actin cytoskeleton organization promotes Gef1 removal from the
412 division site after ring disassembly.

413

414 **Gef1 and Scd1 cooperate to drive polarized cell growth**

415 Since we observed that Gef1 recruits Scd1 at the division site, we addressed whether this
416 crosstalk also instructs Cdc42 at sites of polarized growth. Indeed, we find that Gef1 is

417 necessary for bipolar localization of Scd1 and Scd2. Cells lacking *gef1* are mostly monopolar,
418 with polarized growth occurring only at the old end (Coll et al., 2003; Das et al., 2012). This
419 demonstrates that Gef1 promotes bipolar growth by recruiting Scd1 and Scd2. We report that
420 while constitutively active Cdc42 itself is bipolar, it is not sufficient to restore bipolar localization
421 of Scd1 in *gef1* mutants. This suggests that active Cdc42 alone does not feed into a positive
422 feedback pathway to promote bipolar Scd1 localization. Our findings highlight a requirement for
423 Gef1 in this process. The two ends in fission yeast compete for active Cdc42; the old end is the
424 dominant end and initially wins this competition (Das et al., 2012). Bipolarity is established when
425 the new end overcomes the dominance of the old end and can initiate growth. Thus, the new
426 end is a nascent growth site that must activate Cdc42 in the absence of pre-established cues.
427 Analysis of the growth pattern of *gef1* Δ mutants indicates that new ends frequently fail to
428 overcome old end dominance, resulting in monopolar growth in these cells. Bipolar growth in
429 *gef1* Δ mutants is typically observed in cells that do not contain a dominant old end. Taken
430 together, our findings show that Gef1 allows the new end to overcome old end dominance
431 through Scd1 recruitment and Cdc42 activation, leading to bipolar growth (Figure 7C).
432 *gef1S112A* mutants (Das et al., 2015) and constitutively active Cdc42 mutants, both display
433 bipolar growth. However, only *gef1S112A* mutants display bipolar Scd1 localization in which
434 both the old and the new end recruit Scd1 and initiate growth almost immediately after
435 completion of division. This provides further evidence that Gef1 promotes Scd1 recruitment to
436 initiate bipolar growth.

437 In fission yeast, Scd1 is the primary GEF that promotes polarized growth (Chang et al., 1994).
438 Cells lacking *scd1* are depolarized due to ectopic Cdc42 activation. We find that ectopic Cdc42
439 activation in these mutants is most likely due to mislocalized Gef1. In the presence of *scd1*,
440 Gef1 shows sparse localization and is restricted to the cell ends. Cells lacking *scd1*, fail to
441 restrict Gef1 localization to the ends (Figure 7C). We find that Gef1 is mislocalized in the
442 absence of the actin cytoskeleton, leading to ectopic Cdc42 activation. Furthermore, ectopic
443 Cdc42 activation in LatA-treated cells is abolished in *gef1* Δ mutants. This determines that the
444 ectopic Cdc42 activation observed in LatA-treated cells is Gef1-dependent. Since *scd1* mutants
445 display defects in actin organization, we posit that Scd1 promotes polarized Gef1 localization via
446 the actin cytoskeleton. A recent report shows that ectopic Cdc42 activation in LatA-treated cells
447 depends on the stress-activated MAP kinase Sty1 (Mutavchiev et al., 2016). We found that
448 fission yeast cells treated with LatA did not display ectopic Cdc42 activation in the absence of
449 *sty1*. It is possible that in the absence of actin the cells elicit a stress response, leading to Sty1
450 activation that results in the mislocalization of Gef1. Further analysis will be necessary to test
451 this hypothesis.

452

453 **Multiple GEFs combinatorially regulate Cdc42 during complex processes**

454 The presence of multiple regulators generates combinatorial control that allows for the fine-
455 tuning of a system in different conditions. Furthermore, multiple regulators may interact to
456 instruct each other. Here we report an interesting interplay between Gef1 and Scd1, in which
457 Gef1 promotes Scd1-mediated Cdc42 activation while Scd1 prevents inappropriate Gef1
458 mediated Cdc42 activation. Thus, Gef1 and Scd1 crosstalk establishes and maintains polarized
459 growth. Polarized cell growth requires symmetry breaking, and several models have indicated a
460 need for positive feedback loops in this process (Irazoqui et al., 2003; Kozubowski et al., 2008;
461 Slaughter et al., 2009b). Cdc42 is able to break symmetry and establish polarization through

462 positive feedback (Kozubowski et al., 2008; Slaughter et al., 2009b). Elegant experiments in
463 budding yeast demonstrate that local activation of Cdc42 establishes positive feedback through
464 the recruitment of additional GEFs to amplify the conversion of Cdc42-GDP to Cdc42-GTP
465 (Butty et al., 2002; Kozubowski et al., 2008). We expected Gef1-mediated recruitment of Scd1
466 to function via local activation of Cdc42, which would recruit Scd1 through the establishment of
467 positive feedback. We report that active Cdc42 is not sufficient to recruit Scd1 in the absence of
468 Gef1. While it has been proposed that Cdc42 establishes positive feedback through the
469 formation of the ternary complex consisting of the Cdc42 effector PAK (p21-activated kinases)
470 and its associated scaffold protein (Scd2 or Bem1) (Butty et al., 2002; Kozubowski et al., 2008),
471 studies in *S. pombe* and *S. cerevisiae* suggest that Pak1 kinase activity antagonizes either the
472 Cdc42 scaffold or the GEF, rather than establishing a positive feedback (Das et al., 2012; Gulli
473 et al., 2000; Kuo et al., 2014; Rapali et al., 2017). In support of this antagonistic role of Pak1, we
474 find that more Scd1 accumulates at cell ends and at the division site in the *pak1* switch-off
475 mutant. This indicates that Pak1 does not drive positive feedback, but rather serves to limit the
476 level of Cdc42 activation. Our findings that active Cdc42 failed to recruit Scd1 in the absence of
477 *gef1*, and that Pak kinase antagonizes Scd1, do not agree with current models of Cdc42-
478 mediated positive feedback. This may be due, in part, to the fact that most of these models are
479 based on studies in budding yeast. An alternate hypothesis that can explain our observations is
480 that Cdc42 needs to cycle between an active and an inactive form, to establish a positive
481 feedback and recruit the GEFs. Cycling between the active and inactive forms of Cdc42 was
482 precluded from our studies through the use of the constitutively active *cdc42G12V* allele. This
483 highlights that the mechanisms that generate feedbacks critical to many biological processes
484 merit further investigation.

485 Cdc42 activation undergoes an oscillatory pattern at the cell ends that promotes bipolarity.
486 Current models to explain these oscillations indicate the presence of positive feedback, time-
487 delayed negative feedback, and competition between the two ends for active Cdc42. Since
488 Scd1 is the Cdc42 GEF that establishes polarized growth, we posit that Scd1 activates Cdc42
489 through positive feedback at the dominant old end. Dominance at the old end ensures that Scd1
490 localization is mainly restricted to this end at the expense of the new end. A previous model
491 suggests that as the cell reaches a certain size, a corresponding increase in Scd1 levels would
492 allow the new end to overcome old end dominance to initiate growth and promote bipolarity.
493 Competition for Scd1 alone cannot explain our finding that bipolarity ensues when old end
494 dominance is overcome through Gef1-mediated recruitment of Scd1 to the new end.
495 Furthermore, *gef1S112A* cells display bipolar growth at a smaller cell size. Although an increase
496 in Scd1 levels may promote bipolarity, our data reveal that Gef1-mediated Scd1 recruitment is
497 the more important factor to establish bipolar growth.

498 Our finding that active Cdc42 alone does not promote localization of Scd1 to nascent sites may
499 provide an advantage to the cell. A caveat of a positive feedback model driven solely by active
500 Cdc42 is that any stochastic activation of Cdc42 at the cell cortex may generate random Scd1-
501 mediated growth sites. Our data indicate that active Cdc42 is not sufficient to localize Scd1 to
502 additional sites of growth. Instead, in a cell with a dominant old end, Gef1 must help recruit
503 Scd1 to the new end to allow bipolar growth (Figure 7C). Given that Gef1 promotes Scd1-
504 mediated polarized growth at the new end, it is conceivable that Gef1 itself is tightly regulated to
505 prevent random Cdc42 activation. Indeed, Gef1 shows sparse localization to the cell ends and
506 is mainly cytoplasmic (Das et al., 2015). The NDR kinase Orb6 prevents ectopic Gef1
507 localization via 14-3-3-mediated sequestration to the cytoplasm (Das et al., 2015; Das et al.,

508 2009). Here we show that while Gef1 promotes Scd1 recruitment to a nascent site, Scd1 itself
509 restricts Gef1 localization to the cell ends to precisely activate Cdc42 (Figure 7C). Together our
510 findings describe an elegant system in which the two Cdc42 GEFs regulate each other to
511 ensure proper cell polarization.

512

513 **Significance of GEF coordination in other systems**

514 In budding yeast, CDC24 is required for polarization during bud emergence and is essential for
515 viability (Sloat et al., 1981; Sloat and Pringle, 1978), unlike Scd1 in fission yeast. Budding yeast
516 also has a second GEF Bud3, which establishes a proper bud site (Kang et al., 2014). During
517 G1 in budding yeast, bud emergence occurs via biphasic Cdc42 activation by the two GEFs:
518 Bud3 helps select the bud site (Kang et al., 2014), and Cdc24 allows polarization (Sloat et al.,
519 1981; Sloat and Pringle, 1978). This is analogous to new end growth in fission yeast, which
520 requires Gef1-dependent recruitment of Scd1 for robust Cdc42 activation. It would be interesting
521 to see if crosstalk also exists between Bud3 and Cdc24.

522 The Rho family of GTPases includes Rho, Rac, and Cdc42. In certain mammalian cells, Cdc42
523 and Rac1 appear to activate cell growth in a biphasic manner (de Beco et al., 2018; Yang et al.,
524 2016). For example, during motility, the GTPases, Rho, Rac, and Cdc42, regulate the actin
525 cytoskeleton (Heasman and Ridley, 2008; Machacek et al., 2009). During cell migration, these
526 GTPases form bands or 'zones' in the leading and trailing regions of the cell (Ridley, 2015).
527 Their spatial separation is mediated by the organization of their GEFs and GAPs, as well as by
528 regulatory signaling between these GTPases (Guilluy et al., 2011). Cdc42 and Rho are mutually
529 antagonistic, explaining how such zones of GTPase activity can be established and maintained
530 (Guilluy et al., 2011; Kutys and Yamada, 2014; Warner and Longmore, 2009). Similarly, Cdc42
531 can refine Rac activity (Guilluy et al., 2011). Cdc42 and Rac are activated by similar pathways
532 and share the same effectors. Several recent experiments demonstrate that, during cell
533 migration, reorganization of the actin cytoskeleton occurs in a biphasic manner, where Cdc42
534 activation at new sites sets the direction, while robust Rac activation determines the speed (de
535 Beco et al., 2018; Yang et al., 2016). Unlike most eukaryotes, the genome of *S. pombe* does not
536 contain a Rac GTPase. We speculate that the two Cdc42 GEFs of *S. pombe* allow it to fulfill the
537 roles of both Cdc42 and Rac. Gef1 sets the direction of growth by establishing growth at a new
538 site, while Scd1 promotes efficient growth through robust Cdc42 activation at the growth sites.
539 We propose that the crosstalk between the Cdc42 GEFs themselves is an intrinsic property of
540 small GTPases and is necessary for fine-tuning their activity.

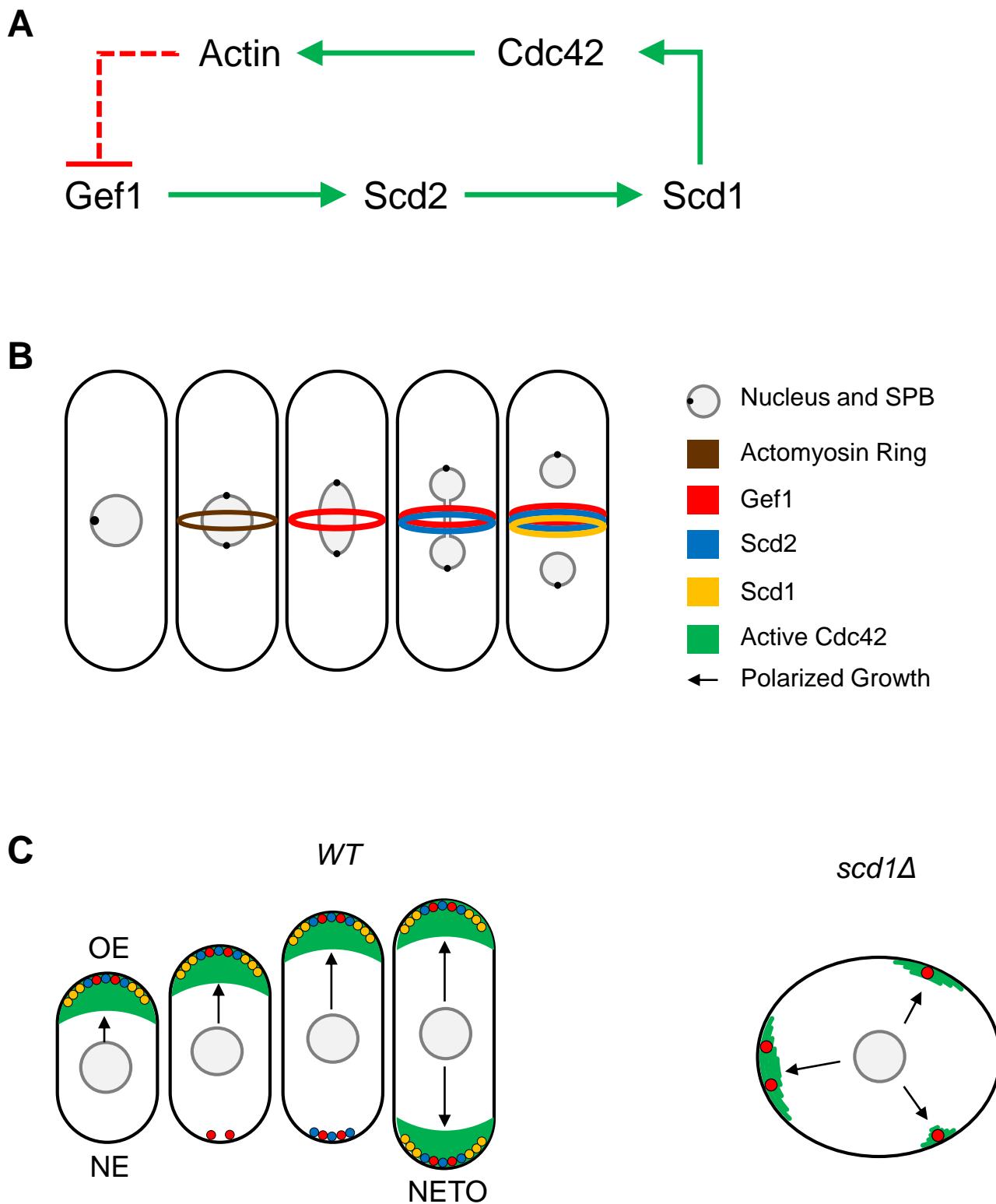


Figure 7

Figure 7: Model of the crosstalk between Gef1 and Scd1 that promotes polarized bipolar growth. **(A)** Diagram of the crosstalk pathway between Gef1 and Scd1. Solid arrows indicate an activating or promoting relationship in the direction of the arrow. Red terminating arrow indicates inactivation or removal of the protein at the arrows terminus. Dashed arrows indicate that the mechanism that regulates the proteins to which these arrows point is not yet resolved. **(B)** Schematic depicting the sequential localization of Gef1, Scd2, and Scd1 to the division site during cytokinesis. At the division site Gef1 localizes first and promotes Scd2 localization. Scd2 at the division site then recruits Scd1. **(C)** Schematic illustrating the crosstalk between Gef1 and Scd1 that promotes bipolar growth and regulates cell shape. In wild type (WT) cells, Gef1 localizes Scd2 to the new end, which in turn recruits Scd1 thus enabling NETO. In *scd1Δ* cells Gef1 localization is no longer restricted to the cell ends leading to ectopic Cdc42 activation and loss of polarity.

541 MATERIALS AND METHODS

542

543 Strains and cell culture

544 The *S. pombe* strains used in this study are listed in Supplemental Table S1. All strains are
545 isogenic to the original strain PN567. Cells were cultured in yeast extract (YE) medium and
546 grown exponentially at 25°C, unless specified otherwise. Standard techniques were used for
547 genetic manipulation and analysis (Moreno et al., 1991). Cells were grown exponentially for at
548 least 3 rounds of eight generations each before imaging.

549

550 Microscopy

551 Cells were imaged at room temperature (23–25°C) with an Olympus IX83 microscope equipped
552 with a VTHawk two-dimensional array laser scanning confocal microscopy system (Visitach
553 International, Sunderland, UK), electron-multiplying charge-coupled device digital camera
554 (Hamamatsu, Hamamatsu City, Japan), and 100x/numerical aperture 1.49 UAPO lens
555 (Olympus, Tokyo, Japan). Images were acquired with MetaMorph (Molecular Devices,
556 Sunnyvale, CA) and analyzed by ImageJ (National Institutes of Health, Bethesda, MD).

557

558 Actin staining

559 The actin cytoskeleton was stained by Alexa Fluor Phalloidin as described here (Das et al.,
560 2009; Pelham and Chang, 2001). Briefly, exponentially growing cells were fixed with 3.5%
561 formaldehyde for 10 minutes at room temperature. The fixed cells were washed with PM buffer
562 (35 mM KPO₄, pH 6.8, 0.5 mM MgSO₄) permeabilized with 1% triton X-100 and stained with
563 Alexa Fluor Phalloidin (Molecular Probes) for 30 minutes.

564

565 Analysis of growth pattern

566 The growth pattern of *gef1+* and *gef1Δ* cells was observed by live imaging of cells through
567 multiple generations. Cells were placed in 3.5-mm glass-bottom culture dishes (MatTek,
568 Ashland, MA) and overlaid with YE medium plus 1% agar, and 100μM ascorbic acid to minimize
569 photo-toxicity to the cell. A bright-field image was acquired every minute for 12 hours. Birth
570 scars were used to distinguish between, as well as to measure, old end and new end growth.

571

572 Construction of fluorescently tagged Gef1 fusion proteins

573 The forward primer 5'-CCCGGGAACCCTCGCAGCTAAAGA-3' with a 5' BamHI site and the
574 reverse primer 5'-GGATCCGTGTTTACCAAAGTTATGTAAGAC-3' with a 5' XmaI site were
575 used to amplify a 3kb DNA fragment containing *gef1*, the 5' UTR, and the endogenous
576 promoter. The fragment was then digested with BamHI and XmaI and ligated into the BamHI-
577 XmaI site of pKS392 pFA6-tdTomato-kanMX and pKG6507 pFA6-mNeonGreen-kanMX.
578 Constructs were linearized by digestion with XbaI and transformed into the *gef1* locus in *gef1Δ*
579 cells.

580

581 Expression of constitutively active Cdc42

582 *pjk148-nmt41x-leu1+* or *pjk148-nmt41x:cdc42G12V-leu1+* were linearized with NdeI and
583 integrated into the *leu1-32* loci in *gef1+* and *gef1Δ* cells expressing either CRIB-3xGFP or Scd1-
584 3xGFP. The empty vector *pjk148-nmt41x-leu1+* was used as control. Cells were grown in YE to
585 promote minimal expression of *cdc42G12V*.

586

587 Latrunculin A treatment

588 Cells in YE were incubated at room temperature with 10 μ M Latrunculin A dissolved in dimethyl
589 sulfoxide (DMSO) for 40 min prior to imaging. Control cells were treated with 1% DMSO and
590 incubated for 40 min.

591

592 **CK666 treatment**

593 Cells in YE were incubated at room temperature with 100 μ M CK666 dissolved in dimethyl
594 sulfoxide (DMSO) for 5 min prior to imaging. Control cells were treated with 1% DMSO and
595 incubated for 5 min.

596

597 **Analysis of fluorescent intensity**

598 Mutants expressing fluorescent proteins were grown to OD 0.5 and imaged on slides. Cells in
599 slides were imaged for no more than 3 minutes to prevent any stress response as previously
600 described (Das et al., 2015). Depending on the mutant and the fluorophore, 16-28 Z-planes
601 were collected at a z-interval of 0.4 μ m for either or both the 488nm and 561nm channels. The
602 respective controls were grown and imaged in an identical manner. ImageJ was used to
603 generate sum projections from the z-series, and to measure the fluorescence intensity of a
604 selected region (actomyosin ring, or growth cap at cell tip). The background fluorescence in a
605 cell-free region of the image was subtracted to generate the normalized intensity. Mean
606 normalized intensity was calculated for each image from all (n>5) measurable cells within each
607 field. A Student's two-tailed t-test, assuming unequal variance, was used to determine
608 significance through comparison of each strain's mean normalized intensities.

609

610 **Acknowledgements**

611 We thank J. Bembenek and T. Burch-Smith for critical review of our manuscript; K. Gould for
612 supplying plasmids; and M. Balasubramanian, and S. Martin for providing strains. This work was
613 supported by a grant from the National Science Foundation (1616495).

614

615 **Competing Interest**

616 The authors do not have any financial and non-financial competing interests.

617 **REFERENCES**

- 618 Atkins, B.D., S. Yoshida, K. Saito, C.F. Wu, D.J. Lew, and D. Pellman. 2013. Inhibition of Cdc42
619 during mitotic exit is required for cytokinesis. *J Cell Biol.* 202:231-240.
- 620 Bendezu, F.O., and S.G. Martin. 2013. Cdc42 explores the cell periphery for mate selection in
621 fission yeast. *Curr Biol.* 23:42-47.
- 622 Bendezu, F.O., V. Vincenzetti, D. Vavylonis, R. Wyss, H. Vogel, and S.G. Martin. 2015.
623 Spontaneous Cdc42 polarization independent of GDI-mediated extraction and actin-
624 based trafficking. *PLoS Biol.* 13:e1002097.
- 625 Bos, J.L., H. Rehmann, and A. Wittinghofer. 2007. GEFs and GAPs: critical elements in the
626 control of small G proteins. *Cell.* 129:865-877.
- 627 Butty, A.C., N. Perrinjaquet, A. Petit, M. Jaquenoud, J.E. Segall, K. Hofmann, C. Zwahlen, and
628 M. Peter. 2002. A positive feedback loop stabilizes the guanine-nucleotide exchange
629 factor Cdc24 at sites of polarization. *EMBO J.* 21:1565-1576.
- 630 Carlin, L.M., R. Evans, H. Milewicz, L. Fernandes, D.R. Matthews, M. Perani, J. Levitt, M.D.
631 Keppler, J. Monypenny, T. Coolen, P.R. Barber, B. Vojnovic, K. Suhling, F. Fraternali, S.
632 Ameer-Beg, P.J. Parker, N.S. Thomas, and T. Ng. 2011. A targeted siRNA screen
633 identifies regulators of Cdc42 activity at the natural killer cell immunological synapse. *Sci*
634 *Signal.* 4:ra81.
- 635 Chang, E.C., M. Barr, Y. Wang, V. Jung, H.P. Xu, and M.H. Wigler. 1994. Cooperative
636 interaction of *S. pombe* proteins required for mating and morphogenesis. *Cell.* 79:131-
637 141.
- 638 Coffman, V.C., J.A. Sees, D.R. Kovar, and J.Q. Wu. 2013. The formins Cdc12 and For3
639 cooperate during contractile ring assembly in cytokinesis. *J Cell Biol.* 203:101-114.
- 640 Coll, P.M., Y. Trillo, A. Ametzazurra, and P. Perez. 2003. Gef1p, a new guanine nucleotide
641 exchange factor for Cdc42p, regulates polarity in *Schizosaccharomyces pombe*.
642 *Molecular biology of the cell.* 14:313-323.
- 643 Crawford, J.M., N. Harden, T. Leung, L. Lim, and D.P. Kiehart. 1998. Cellularization in
644 *Drosophila melanogaster* is disrupted by the inhibition of rho activity and the activation of
645 Cdc42 function. *Dev Biol.* 204:151-164.
- 646 Das, M., T. Drake, D.J. Wiley, P. Buchwald, D. Vavylonis, and F. Verde. 2012. Oscillatory
647 Dynamics of Cdc42 GTPase in the Control of Polarized Growth. *Science.*
- 648 Das, M., I. Nunez, M. Rodriguez, D.J. Wiley, J. Rodriguez, A. Sarkeshik, J.R. Yates, 3rd, P.
649 Buchwald, and F. Verde. 2015. Phosphorylation-dependent inhibition of Cdc42 GEF
650 Gef1 by 14-3-3 protein Rad24 spatially regulates Cdc42 GTPase activity and oscillatory
651 dynamics during cell morphogenesis. *Mol Biol Cell.*
- 652 Das, M., and F. Verde. 2013. Role of Cdc42 dynamics in the control of fission yeast cell
653 polarization. *Biochem Soc Trans.* 41:1745-1749.

- 654 Das, M., D.J. Wiley, X. Chen, K. Shah, and F. Verde. 2009. The conserved NDR kinase Orb6
655 controls polarized cell growth by spatial regulation of the small GTPase Cdc42. *Curr*
656 *Biol.* 19:1314-1319.
- 657 de Beco, S., K. Vaidziulyte, J. Manzi, F. Dalier, F. Di Frederico, G. Cornilleau, M. Dahan, and M.
658 Coppey. 2018. Optogenetic dissection of Rac1 and Cdc42 gradient shaping. *bioRxiv*.
- 659 Drubin, D.G., and W.J. Nelson. 1996. Origins of cell polarity. *Cell.* 84:335-344.
- 660 Dutartre, H., J. Davoust, J.P. Gorvel, and P. Chavrier. 1996. Cytokinesis arrest and
661 redistribution of actin-cytoskeleton regulatory components in cells expressing the Rho
662 GTPase CDC42Hs. *J Cell Sci.* 109 (Pt 2):367-377.
- 663 Endo, M., M. Shirouzu, and S. Yokoyama. 2003. The Cdc42 binding and scaffolding activities of
664 the fission yeast adaptor protein Scd2. *J Biol Chem.* 278:843-852.
- 665 Estravis, M., S. Rincon, and P. Perez. 2012. Cdc42 regulation of polarized traffic in fission
666 yeast. *Commun Integr Biol.* 5:370-373.
- 667 Estravis, M., S.A. Rincon, B. Santos, and P. Perez. 2011. Cdc42 regulates multiple membrane
668 traffic events in fission yeast. *Traffic.* 12:1744-1758.
- 669 Etienne-Manneville, S. 2004. Cdc42--the centre of polarity. *Journal of cell science.* 117:1291-
670 1300.
- 671 Feierbach, B., and F. Chang. 2001. Roles of the fission yeast formin for3p in cell polarity, actin
672 cable formation and symmetric cell division. *Current biology : CB.* 11:1656-1665.
- 673 Feigin, M.E., and S.K. Muthuswamy. 2009. Polarity proteins regulate mammalian cell-cell
674 junctions and cancer pathogenesis. *Curr Opin Cell Biol.* 21:694-700.
- 675 Gachet, Y., and J.S. Hyams. 2005. Endocytosis in fission yeast is spatially associated with the
676 actin cytoskeleton during polarised cell growth and cytokinesis. *J Cell Sci.* 118:4231-
677 4242.
- 678 Godde, N.J., R.C. Galea, I.A. Elsum, and P.O. Humbert. 2010. Cell polarity in motion: redefining
679 mammary tissue organization through EMT and cell polarity transitions. *J Mammary*
680 *Gland Biol Neoplasia.* 15:149-168.
- 681 Guilluy, C., R. Garcia-Mata, and K. Burridge. 2011. Rho protein crosstalk: another social
682 network? *Trends Cell Biol.* 21:718-726.
- 683 Gulli, M.P., M. Jaquenoud, Y. Shimada, G. Niederhauser, P. Wiget, and M. Peter. 2000.
684 Phosphorylation of the Cdc42 exchange factor Cdc24 by the PAK-like kinase Cla4 may
685 regulate polarized growth in yeast. *Mol Cell.* 6:1155-1167.
- 686 Halaoui, R., and L. McCaffrey. 2014. Rewiring cell polarity signaling in cancer. *Oncogene.*
- 687 Harris, K.P., and U. Tepass. 2010. Cdc42 and vesicle trafficking in polarized cells. *Traffic.*
688 11:1272-1279.

- 689 Heasman, S.J., and A.J. Ridley. 2008. Mammalian Rho GTPases: new insights into their
690 functions from in vivo studies. *Nat Rev Mol Cell Biol.* 9:690-701.
- 691 Hirota, K., K. Tanaka, K. Ohta, and M. Yamamoto. 2003. Gef1p and Scd1p, the Two GDP-GTP
692 exchange factors for Cdc42p, form a ring structure that shrinks during cytokinesis in
693 *Schizosaccharomyces pombe*. *Mol Biol Cell.* 14:3617-3627.
- 694 Howell, A.S., M. Jin, C.F. Wu, T.R. Zyla, T.C. Elston, and D.J. Lew. 2012. Negative feedback
695 enhances robustness in the yeast polarity establishment circuit. *Cell.* 149:322-333.
- 696 Huang, J., Y. Huang, H. Yu, D. Subramanian, A. Padmanabhan, R. Thadani, Y. Tao, X. Tang,
697 R. Wedlich-Soldner, and M.K. Balasubramanian. 2012. Nonmedially assembled F-actin
698 cables incorporate into the actomyosin ring in fission yeast. *J Cell Biol.* 199:831-847.
- 699 Hwang, J.U., Y. Gu, Y.J. Lee, and Z. Yang. 2005. Oscillatory ROP GTPase activation leads the
700 oscillatory polarized growth of pollen tubes. *Mol Biol Cell.* 16:5385-5399.
- 701 Irazoqui, J.E., A.S. Gladfelter, and D.J. Lew. 2003. Scaffold-mediated symmetry breaking by
702 Cdc42p. *Nat Cell Biol.* 5:1062-1070.
- 703 Johnson, D.I. 1999. Cdc42: An essential Rho-type GTPase controlling eukaryotic cell polarity.
704 *Microbiology and molecular biology reviews : MMBR.* 63:54-105.
- 705 Kang, P.J., M.E. Lee, and H.O. Park. 2014. Bud3 activates Cdc42 to establish a proper growth
706 site in budding yeast. *J Cell Biol.* 206:19-28.
- 707 Kelly, F.D., and P. Nurse. 2011. Spatial control of Cdc42 activation determines cell width in
708 fission yeast. *Mol Biol Cell.* 22:3801-3811.
- 709 Kozubowski, L., K. Saito, J.M. Johnson, A.S. Howell, T.R. Zyla, and D.J. Lew. 2008. Symmetry-
710 breaking polarization driven by a Cdc42p GEF-PAK complex. *Current biology : CB.*
711 18:1719-1726.
- 712 Kuo, C.C., N.S. Savage, H. Chen, C.F. Wu, T.R. Zyla, and D.J. Lew. 2014. Inhibitory GEF
713 phosphorylation provides negative feedback in the yeast polarity circuit. *Curr Biol.*
714 24:753-759.
- 715 Kutys, M.L., and K.M. Yamada. 2014. An extracellular-matrix-specific GEF-GAP interaction
716 regulates Rho GTPase crosstalk for 3D collagen migration. *Nat Cell Biol.* 16:909-917.
- 717 Lauffenburger, D.A., and A.F. Horwitz. 1996. Cell migration: a physically integrated molecular
718 process. *Cell.* 84:359-369.
- 719 Machacek, M., L. Hodgson, C. Welch, H. Elliott, O. Pertz, P. Nalbant, A. Abell, G.L. Johnson,
720 K.M. Hahn, and G. Danuser. 2009. Coordination of Rho GTPase activities during cell
721 protrusion. *Nature.* 461:99-103.
- 722 Martin, S.G., S.A. Rincon, R. Basu, P. Perez, and F. Chang. 2007. Regulation of the formin
723 for3p by cdc42p and bud6p. *Molecular biology of the cell.* 18:4155-4167.

- 724 Mitchison, J.M., and P. Nurse. 1985. Growth in cell length in the fission yeast
725 *Schizosaccharomyces pombe*. *Journal of cell science*. 75:357-376.
- 726 Moreno, S., A. Klar, and P. Nurse. 1991. Molecular genetic analysis of fission yeast
727 *Schizosaccharomyces pombe*. *Methods in enzymology*. 194:795-823.
- 728 Mutavchiev, D.R., M. Leda, and K.E. Sawin. 2016. Remodeling of the Fission Yeast Cdc42 Cell-
729 Polarity Module via the Sty1 p38 Stress-Activated Protein Kinase Pathway. *Curr Biol*.
730 26:2921-2928.
- 731 Nabeshima, K., T. Nakagawa, A.F. Straight, A. Murray, Y. Chikashige, Y.M. Yamashita, Y.
732 Hiraoka, and M. Yanagida. 1998. Dynamics of centromeres during metaphase-anaphase
733 transition in fission yeast: Dis1 is implicated in force balance in metaphase bipolar
734 spindle. *Mol Biol Cell*. 9:3211-3225.
- 735 Nance, J., and J.A. Zallen. 2011. Elaborating polarity: PAR proteins and the cytoskeleton.
736 *Development*. 138:799-809.
- 737 Onishi, M., N. Ko, R. Nishihama, and J.R. Pringle. 2013. Distinct roles of Rho1, Cdc42, and
738 Cyk3 in septum formation and abscission during yeast cytokinesis. *J Cell Biol*. 202:311-
739 329.
- 740 Pelham, R.J., and F. Chang. 2001. Role of actin polymerization and actin cables in actin-patch
741 movement in *Schizosaccharomyces pombe*. *Nature cell biology*. 3:235-244.
- 742 Pollard, T.D. 2010. Mechanics of cytokinesis in eukaryotes. *Curr Opin Cell Biol*. 22:50-56.
- 743 Rapali, P., R. Mitteau, C. Braun, A. Massoni-Laporte, C. Unlu, L. Bataille, F.S. Arramon, S.P.
744 Gygi, and D. McCusker. 2017. Scaffold-mediated gating of Cdc42 signalling flux. *Elife*. 6.
- 745 Ridley, A.J. 2006. Rho GTPases and actin dynamics in membrane protrusions and vesicle
746 trafficking. *Trends Cell Biol*. 16:522-529.
- 747 Ridley, A.J. 2015. Rho GTPase signalling in cell migration. *Curr Opin Cell Biol*. 36:103-112.
- 748 Sit, S.T., and E. Manser. 2011. Rho GTPases and their role in organizing the actin cytoskeleton.
749 *J Cell Sci*. 124:679-683.
- 750 Slaughter, B.D., A. Das, J.W. Schwartz, B. Rubinstein, and R. Li. 2009a. Dual modes of cdc42
751 recycling fine-tune polarized morphogenesis. *Developmental cell*. 17:823-835.
- 752 Slaughter, B.D., S.E. Smith, and R. Li. 2009b. Symmetry breaking in the life cycle of the
753 budding yeast. *Cold Spring Harbor Perspect Biol*. 1:a003384.
- 754 Sloat, B.F., A. Adams, and J.R. Pringle. 1981. Roles of the CDC24 gene product in cellular
755 morphogenesis during the *Saccharomyces cerevisiae* cell cycle. *J Cell Biol*. 89:395-405.
- 756 Sloat, B.F., and J.R. Pringle. 1978. A mutant of yeast defective in cellular morphogenesis.
757 *Science*. 200:1171-1173.
- 758 Spector, I., N.R. Shochet, Y. Kashman, and A. Groweiss. 1983. Latrunculins: novel marine
759 toxins that disrupt microfilament organization in cultured cells. *Science*. 219:493-495.

- 760 Sun, S.C., Z.B. Wang, Y.N. Xu, S.E. Lee, X.S. Cui, and N.H. Kim. 2011. Arp2/3 complex
761 regulates asymmetric division and cytokinesis in mouse oocytes. *PLoS One*. 6:e18392.
- 762 Wang, N., I.J. Lee, G. Rask, and J.Q. Wu. 2016. Roles of the TRAPP-II Complex and the
763 Exocyst in Membrane Deposition during Fission Yeast Cytokinesis. *PLoS Biol*.
764 14:e1002437.
- 765 Warner, S.J., and G.D. Longmore. 2009. Cdc42 antagonizes Rho1 activity at adherens
766 junctions to limit epithelial cell apical tension. *J Cell Biol*. 187:119-133.
- 767 Wedlich-Soldner, R., S.C. Wai, T. Schmidt, and R. Li. 2004. Robust cell polarity is a dynamic
768 state established by coupling transport and GTPase signaling. *J Cell Biol*. 166:889-900.
- 769 Wei, B., B.S. Hercyk, N. Mattson, A. Mohammadi, J. Rich, E. DeBruyne, M.M. Clark, and M.
770 Das. 2016. Unique spatiotemporal activation pattern of Cdc42 by Gef1 and Scd1
771 promotes different events during cytokinesis. *Mol Biol Cell*. 27:1235-1245.
- 772 Wu, J.Q., J.R. Kuhn, D.R. Kovar, and T.D. Pollard. 2003. Spatial and temporal pathway for
773 assembly and constriction of the contractile ring in fission yeast cytokinesis. *Dev Cell*.
774 5:723-734.
- 775 Yang, H.W., S.R. Collins, and T. Meyer. 2016. Locally excitable Cdc42 signals steer cells during
776 chemotaxis. *Nat Cell Biol*. 18:191-201.
- 777